

Functional imaging: new views on lens structure and function

Paul J. Donaldson, Angus C. Grey, B. Rachele Merriman-Smith, A.M.G. Sisley,
Christian Soeller, Mark B. Cannell & Marc D. Jacobs

*Department of Physiology, School of Medical Sciences,
The University of Auckland, Auckland, New Zealand*

Summary

1. We have developed an experimental imaging approach that allows the distribution of lens membrane proteins to be mapped with subcellular resolution over large distances, as a function of fibre cell differentiation.

2. Using this approach in the rat lens, we have precisely localised histological sites of Cx46 cleavage, quantitatively mapped changes in gap junction distribution and fibre cell morphology, and correlated these changes to differences in intercellular dye transfer.

3. Profiling of glucose transporter isoform expression showed that lens epithelial cells express GLUT1 while deeper, cortical fibre cells express the higher-affinity GLUT3 isoform. Near the lens periphery, GLUT3 was located in the cytoplasm of fibre cells, but it underwent a differentiation-dependent membrane insertion.

4. Similarly, the putative adhesion protein MP20 is inserted into the fibre cell membranes, at the stage when the cells lose their nuclei. This redistribution is strikingly rapid in terms of fibre cell differentiation and correlates with a barrier to extracellular diffusion.

5. Our imaging-oriented approach has facilitated new insights into the relationships between fibre cell differentiation and lens function. Taken together, our results indicate that a number of strategies are utilised by the lens during the course of normal differentiation, to change the subcellular distribution, gross spatial location and functional properties of key membrane transport proteins.

Introduction

The transparency of the lens is closely linked to the unique structure and function of its fibre cells. These highly differentiated cells are derived from equatorial epithelial cells, which exit the cell cycle and embark upon a differentiation process that produces extensive cellular elongation, the loss of cellular organelles and nuclei and the expression of fibre-specific proteins^{1,2}. Since this process continues throughout life, a gradient of fibre cells at different stages of differentiation is established around an internalised core of mature, anucleate fibre cells. To maintain its structural organization, and hence, its transparency, the lens is believed to have an internal microcirculation system that delivers nutrients, removes waste products, and imposes the negative membrane potential required to maintain the steady-state volume of the

fibre cells³. This system is thought to be generated by spatial differences in ion transport processes that generate a circulating flux of ions which enters the lens via the extracellular clefts between fibre cells, crosses fibre cell membranes, then flows from cell to cell towards the surface of the lens, via an intracellular pathway mediated by gap junction channels. This circulating current creates a net flux of solute that generates fluid flow. The extracellular flow of water conveys nutrients toward the deeper-lying fibre cells, while the intracellular flow removes wastes and creates a well-stirred intracellular compartment.

The experimental evidence in support of this model of lens circulation has primarily been provided by macroscopic measurements of whole-lens electrical properties³. More recently, our laboratory has provided additional evidence in favour of the model by identifying, and localising at the cellular level, key components of the circulation system⁴. This work has involved a number of functional imaging approaches which correlate membrane protein distribution to function in spatially distinct regions of the lens⁵⁻⁸. Here we compare and contrast the results obtained for three diverse types of membrane proteins: cell-to-cell channel proteins (connexins); glucose transporter proteins (GLUTs); and an adhesion protein (MP20). While our initial goal was to provide a molecular inventory of key components of the lens circulation system, our results have revealed that the lens uses a number of different strategies to establish and maintain spatial differences in membrane transport proteins during the course of fibre cell differentiation.

Mapping spatial differences in transport proteins: a question of scale

To investigate these questions we have developed an experimental approach that allows the distribution of lens membrane proteins to be mapped with subcellular resolution over large distances. Since fibre cells continually differentiate from epithelial cells at the lens periphery and are progressively internalised with age, the spatial layout of fibre cells from the lens periphery to the centre also represents a temporal profile of fibre cell differentiation. The technical procedures we have developed⁹ to map membrane protein distributions across this differentiation gradient, utilize high-quality cryosections that are systematically imaged to produce a continuous, high-resolution data set (Figure 1). Such an image data set contains information not only on how the gross spatial distribution of a labeled membrane protein changes as a

function of fibre cell differentiation, but also on the changing subcellular distribution of the protein (Figure 2). This is important because differentiating fibre cells are essentially elongated epithelial cells, which retain distinct apical, basal and lateral membrane domains¹⁰. In these cells the lateral membranes are further divided into broad and narrow sides, which contribute to the distinctive hexagonal profile of the fibre cells. Thus in addition to radial differences in membrane protein distribution which can occur as a consequence of fibre cell differentiation, other changes may be evident in an axial direction (pole-equator-pole) along the length of a fibre cell or between the lateral membrane domains (broad versus narrow side).

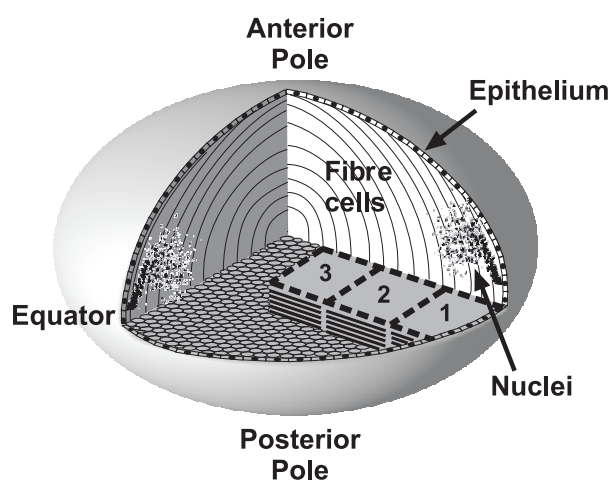


Figure 1. High-resolution long-range imaging in the lens. This diagram illustrates our application of quantitative two-photon, and confocal imaging in the equatorial region of the lens. Overlapping, large image stacks (1-3) can be collected from high-quality cryosections at diffraction-limited resolution, and precisely aligned by correlation analysis⁹ to form a continuous 3D data set spanning a large proportion of the lens radius (see Figure 2). Expression patterns of immunofluorescence-labeled proteins can be examined qualitatively by extracting high-magnification views from exact locations within the data set, or analyzed quantitatively as a function of fibre cell age using custom-written image processing software. Fibre cell nuclei disperse axially (i.e. toward the poles) and degrade as the cells age, providing a convenient differentiation marker when stained with a DNA-binding fluorochrome such as propidium iodide. Nuclear degradation, and protein expression in fibre cell lateral membrane domains, can be precisely localised in equatorial sections showing transverse views of fibre cells. Nuclear dispersal, degradation and longitudinal protein expression patterns, can be localised in axial sections showing the fibre cell lengths.

Fibre cell gap junctions: structure, dispersal and age-dependent processing

Because of their central importance to lens function, the fibre cell gap junctions have been extensively studied¹¹. Gap junctions are formed by the connexin family of proteins¹² and lens fibre cells express two connexin isoforms, Cx46¹³ and Cx50¹⁴. Functional studies indicate that the density of gap junctions is highest near the equator of the lens so as to direct the outward component of the circulating current to the equatorial epithelial cells, which contain the highest density of Na/K pumps¹⁵. Qualitative assessments showed that in the young, equatorial fibre cells, gap junctions are particularly concentrated on the broad sides while in older, inner fibre cells, the gap junctions are more evenly distributed throughout the cell membrane.¹⁶⁻¹⁸ Furthermore, biochemical studies have shown that the cytoplasmic tails of Cx46¹⁹ and Cx50^{20,21} are cleaved in the lens, the latter by the protease calpain²¹, in order to maintain cell coupling at low pH deep in the lens²².

In a more recent study which utilised our high-resolution imaging techniques, we have precisely localised the histological sites of Cx46 cleavage, by quantitative analysis of signal density profiles obtained from antibodies directed against the cytoplasmic loop and tail of Cx46⁸. Our analysis revealed that Cx46 cleavage occurs at two distinct stages during fibre cell differentiation (Figure 3A). The major stage occurs at a normalized radial distance (r/a) ~ 0.9 in 3-week-old lenses, and coincides with an axial dispersal of fibre cell nuclei; the second stage occurs at $r/a \sim 0.7$ and is associated with the complete loss of fibre cell nuclei.

In addition to Cx46 cleavage, we have quantitatively mapped the changing gap junction distributions (Figure 2A-C) as a function of fibre cell differentiation. Radial changes in cell shape and gap junction plaque size and distribution were measured automatically by quantitative morphometric analysis of our image data⁸. A fibre cell 'ellipticity index' was found to increase smoothly from the lens periphery inward, reflecting a gradual change from the hexagonal peripheral cell cross-section to a more circular cross-section. We also quantified a rapid peripheral decrease in the size of broad side plaques which is followed by an apparent fragmentation and dispersal of the plaques around the cell perimeter. These precise radial measurements of fibre cell changes show that the sudden gap junction cleavage and shrinkage events do not correspond to sudden changes in cellular morphology. However, the loss of the hexagonal cell profile is closely associated with gap junction plaque dispersal, and both follow the major stage of Cx46 cleavage, suggesting a possible role for cleavage in gap junction and cell remodeling⁸.

To investigate the functional consequences of these changes, we performed two-photon flash photolysis (TPFP) on lenses loaded with CMNB-caged fluorescein and assessed regional gap junction coupling patterns⁸. By applying TPFP inside a single fibre cell, a microscopic source of uncaged fluorescein was created and its diffusion to neighbouring cells was monitored by simultaneous

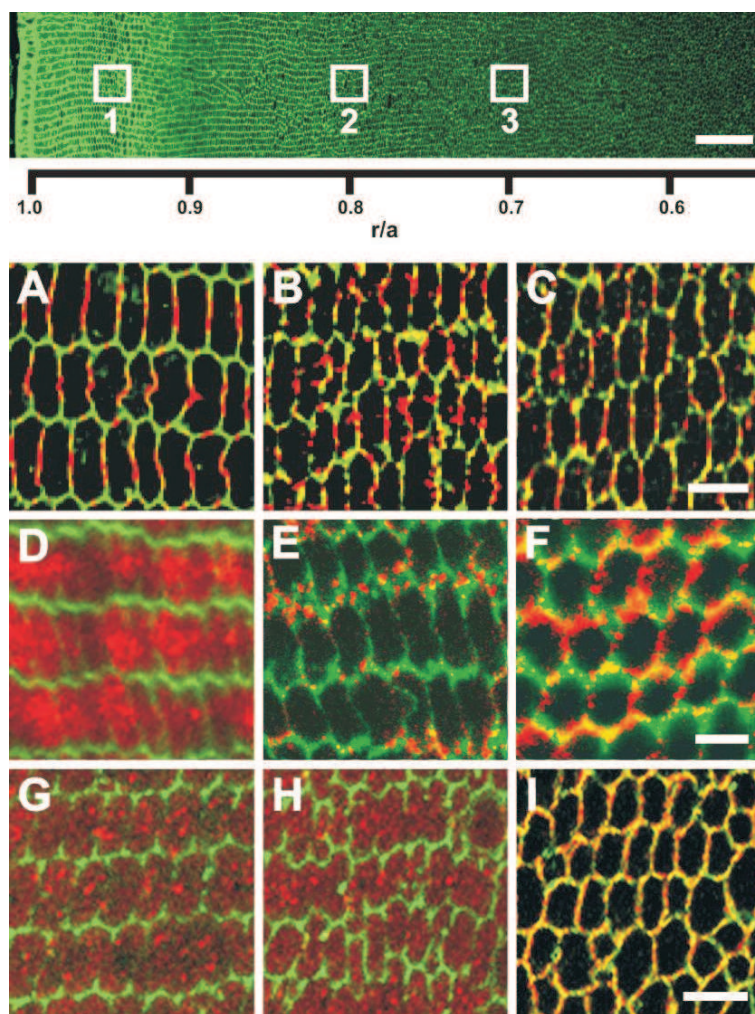


Figure 2. Differentiation-dependent changes in the subcellular distribution of 3 diverse lens proteins.

Top: Four 1024 x 1024 image stacks were assembled as described (Figure 1) to form a continuous, high-resolution immunofluorescence data set extending over half the rat lens radius. The image shows cell membranes labeled with wheat germ agglutinin conjugated to AlexaFluor 350. High-magnification images of the proteins (A-I) were extracted from the approximate locations designated with white boxes to view changes in their distribution as a function of fibre cell age.

A-C: The gap junction protein Cx46 forms large plaques on the broad sides of fibre cells near the lens periphery, with small punctate plaques on the narrow sides (A). As fibre cells age they become rounder, the large plaques become smaller (B), and they fragment and disperse around the cell membrane by the time they reach $r/a \sim 0.7$ (C).

D-F: The GLUT3 glucose transporter protein labels the cytoplasm of peripheral fibre cells (D) but this signal re-locates predominantly to the narrow sides of the cells by $r/a \sim 0.8$ (E); later, at $r/a \sim 0.7$, GLUT3 signal is widely distributed around the rounded fibre cell membranes.

G-I: The membrane protein MP20 is distributed in a granular pattern resembling cytoplasmic vesicles, from the lens periphery to $r/a \sim 0.7$ (G, H), where it is rapidly targeted to the plasma membrane (I). Scale bars: Top, 50 μm ; A-C, D-F and G-I, 5 μm .

confocal microscopy. These experiments revealed different patterns of cell-cell coupling at different radial locations. In peripheral fibre cells, where large broad side plaques predominate, dye diffusion occurred primarily in a radial direction (Figure 3B). In contrast, at locations beyond the zone of nuclear loss, where plaques were distributed more evenly around the fibre cell membrane, the pattern of fluorescein diffusion was approximately isotropic (Figure 3C). Thus the local pattern of intercellular coupling changed from a radial direction in the lens periphery to a

more uniform pattern in the deeper fibre cells, consistent with the differentiation-dependent remodeling of gap junction plaques. It appears, then, that the structure of gap junctions is modified by precise connexin processing and plaque remodeling, which create functional specializations in sub-regions of the organ and allow the maintenance of lens circulation, homeostasis and transparency.

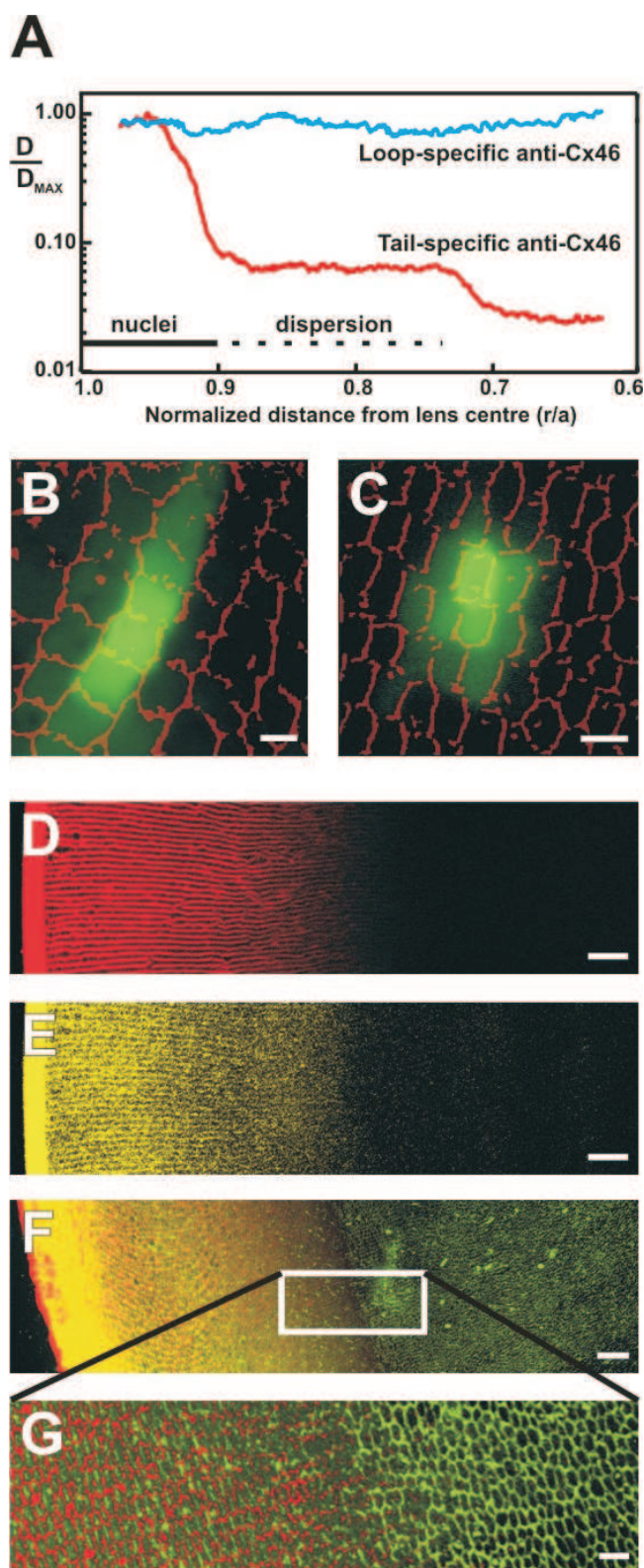


Figure 3. Novel insights gained from an image-based approach to lens function.

A: Precise in situ localization of two cleavage zones of Cx46, in relation to fibre cell differentiation markers. Two antibodies, specific to the cytoplasmic loop or the carboxy terminus ‘tail’ of Cx46, were used to label rat lens sections by immunofluorescence. Fluorescence signal density was imaged and quantified using a two-photon microscope and custom-written software. The density of membrane signal from the Cx46 tail antibody declined rapidly in two discrete zones located at $r/a \sim 0.9$ and ~ 0.7 , while the Cx46 loop antibody signal remained relatively constant, indicating cleavage of the carboxy tail in the two zones, with retention of the rest of the protein in the membrane. The solid and dotted horizontal lines designate the locations of axially clustered or dispersed fibre cell nuclei, respectively, preceding complete nuclear degradation.

B, C: Position-dependent patterns of local cell-cell coupling in the rat lens revealed by dye transfer. Two-photon flash photolysis was used to optically release caged fluorescein within individual fibre cells. Simultaneous confocal imaging of the time course of dye diffusion revealed that cell coupling was predominantly in a radial direction at the lens periphery (**B**) but was more isotropic deep in the lens ($r/a < 0.7$; **C**). These patterns correlate with the sub-cellular distributions of gap junction channels in the respective areas.

D, E: Restricted dye diffusion into the lens. Cultured rat lenses were incubated for 4 hours in Texas Red-dextran (**D**) or Lucifer yellow (**E**), then fixed, sectioned and imaged. Both dyes penetrated the lens via the extracellular space to a depth of only $\sim 400 \mu\text{m}$, corresponding to the zone of nuclear degradation.

F, G: Antibodies to MP20 were applied to lens sections following dye treatment as in (**D**) for 18 hours. Immunofluorescent imaging of the sections showed that localization of MP20 to the cell membranes occurs at a depth corresponding to the limit of extracellular dye diffusion (**F**: red, Texas Red-dextran; green, MP20; **G**: high-magnification view), suggesting a possible role for MP20 in this ‘diffusion barrier’. Scale bars: **B, C**, $5 \mu\text{m}$; **D-F**, $50 \mu\text{m}$; **G**, $10 \mu\text{m}$.

Glucose transporters: differential expression and membrane insertion

Glucose is the principal fuel used by the lens to support growth and homeostasis²³. In the lens, epithelial

and differentiating fibre cells are capable of oxidative phosphorylation, while the mature fibre cells, having lost their mitochondria, must rely solely on glycolysis for energy production². The lens is bathed by the aqueous humor, which contains glucose levels that mirror those in

the plasma. Hence, lens cells near the periphery have access to an abundant supply of glucose, while the supply of glucose to the deeper-lying fibre cells is likely to be limited by a decreasing glucose gradient. However, the circulating current is thought to create a net flux of solutes that generates an extracellular fluid flow^{4,17}, which in turn conveys nutrients toward the deeper-lying fibre cells by advection. Thus, from the model one might predict that both the peripheral and deeper-lying cells would be exposed to external glucose, though at different concentrations, and might express glucose transporters. To address this issue we performed a molecular profiling of GLUT isoform expression in the rat lens²⁴. We found that epithelial cells express GLUT1 while cortical fibre cells express the higher-affinity GLUT3 isoform. This differential expression pattern is consistent with the probable glucose environments these cells are exposed to. In epithelial cells, the expression of GLUT1 appears to determine that the K_m of the glucose transporter is appropriate for the glucose concentration in the aqueous humor. In cortical fibre cells, the lower K_m of GLUT3 is likely to be more appropriate for extracting glucose from the extracellular fluid, which at this distance into the lens should have a relatively low glucose concentration.

Subsequent analysis of GLUT3 expression using our high-resolution image mapping approach revealed an intriguing pattern. Near the lens periphery, GLUT3 was located in the cytoplasm of fibre cells (Figure 2D); but with increasing depth into the lens, GLUT3 labeling became associated with the membrane, suggesting that GLUT3 undergoes a differentiation-dependent membrane insertion⁵. Interestingly, this membrane insertion of GLUT3 was initially targeted to the narrow sides of fibre cell membranes (Figure 2E). Then at a later stage of fibre cell differentiation, GLUT3 became more uniformly dispersed around the entire cell membrane (Figure 2F). The dispersal of GLUT3 from the narrow sides to the rest of the membrane appears to coincide with dispersal of the gap junction plaques which are initially located on the broad sides of fibre cells (Figure 2A-C). This observation reinforces our impression that the distinct sub-domains of fibre cell lateral membranes are lost during the course of differentiation. Our findings also suggest that GLUT3 is initially produced in the younger, peripheral fibre cells (which are capable of protein synthesis) and can be stored in the cytoplasm until a differentiation-dependent signal triggers its insertion into the membrane.

Fibre cell adhesion: MP20 membrane insertion and extracellular diffusion

Membrane insertion would appear to be a common phenomenon in the lens. High-resolution mapping of the distribution of the second most abundant lens membrane protein, MP20, revealed that like GLUT3 it undergoes a differentiation-dependent membrane insertion. Despite its relative abundance, the function of MP20 in the lens is still not definitively known. MP20 has been implicated as a component of membrane junctions between lens fibre

cells^{19,25}, and more recently it was shown that MP20 acts as a ligand for galectin-3²⁶, a known modulator of cell-cell adhesion in other tissues²⁷. These results are consistent with a role for MP20 in cell-cell adhesion, however, the precise role of MP20 in lens structure, and its impact on lens function, have yet to be determined.

Using image-based immunofluorescent mapping, we assessed the relative distributions of MP20 and another abundant membrane protein, the water channel AQP0, as a function of fibre cell differentiation. We found that MP20, but not AQP0, is inserted into the fibre cell membranes at the stage when the cells lose their nuclei⁶. We showed that while MP20 labeling is intracellular in the younger fibre cells of the cortex, it redistributes to the plasma membranes as the cells mature (Figure 2G-I). Furthermore, the redistribution from the cytoplasm to the plasma membrane is relatively rapid and occurs over a small number of cell layers. If MP20 is indeed an adhesion molecule then the insertion of MP20 into the membranes of mature fibre cells might be expected to increase adhesion between the cells. This suggested to us the possibility that upon insertion of MP20, the extracellular space might become effectively smaller or more tortuous, restricting extracellular diffusion of molecules deeper into the lens. To test this hypothesis, we organ-cultured lenses in the presence of two fluorescent extracellular space markers, Texas Red-dextran (MW 10 kDa) and Lucifer yellow (MW 456 Da), for varying times. Regardless of the incubation period (2 to 18 hours), Texas Red-dextran diffusion into the lens only occurred up to a distance of some 400 μm in from the capsule (Figure 3D). This consistency in the depth of tracer penetration observed at all time points indicated that the Texas Red-dextran movement via the extracellular space was not diffusion-limited, but restricted by a physical barrier. In support of this, the extracellular diffusion of the smaller molecular weight dye, Lucifer yellow, also became restricted at around the same depth (Figure 3E). This indicates that the barrier to extracellular diffusion has a molecular weight cut-off of at most ~ 450 Da. Subsequent immunolabelling with MP20 antibodies of sections derived from a lens incubated in Texas Red-dextran for 18 hours indicated that the barrier to extracellular diffusion coincides with the zone where MP20 is inserted into the membrane (Figure 3F, G). Thus the insertion of MP20 correlates with the formation of a diffusion barrier that restricts the further extracellular movement of tracer dye molecules into the lens core. These results are consistent with the view that membrane insertion of MP20 contributes to the establishment of interactions between adjacent fibre cells, which act in the lens to limit the movement of molecules via the extracellular space.

Conclusions and future challenges

Our adoption of a functional imaging approach to investigate key components of the lens microcirculation system has reaped unforeseen insights into lens biology. It appears that the lens adopts a number of strategies to compensate for the inability of its older anucleate fibre cells to synthesise new membrane proteins. These strategies

involve the processing, redistribution and differential targeting of proteins as fibre cells age. The gap junction proteins Cx46 and Cx50 undergo specific, differentiation-dependent post-translational modifications that remove their cytoplasmic tails: events which cause a loss of junctional pH sensitivity and which bracket (temporally and spatially) a dramatic redistribution of gap junction plaques. This redistribution correlates with a major redirection of the local cell-cell coupling which underpins the lens microcirculation system. In a similar vein, the differentiation-dependent expression of glucose transporters, which targets the GLUT1 isoform to epithelial cells and the GLUT3 isoform to cortical cells, appears to match transporter affinity with local glucose availability. In order to achieve this, GLUT3 undergoes insertion into fibre cell narrow side membranes, apparently from a pre-designated cytoplasmic pool. Like GLUT3, MP20 also undergoes a membrane insertion event, but at a later stage of fibre cell differentiation, suggesting that the signals responsible for the insertion of these two membrane proteins are different. Insertion of MP20 correlates with the formation of an extracellular diffusion barrier. Taken together, our results show that as fibre cells mature and their ability to synthesise new membrane proteins is lost, the lens deploys a panoply of post-translational processing and targeting mechanisms to enable fibre cells to meet the physiological challenges associated with being buried ever deeper in the lens mass.

Since the lens is continually adding new fibre cells at its equator, it is interesting to speculate that establishing and maintaining spatial differences in membrane transport proteins is an integral part of the fibre cell differentiation programme. Having developed image-based methods to precisely map, with high resolution, spatial changes in membrane protein distribution, the next challenge is to identify the differentiation signals that trigger the very precise changes we have observed. If this is achieved, the lens will not only be an excellent model system in which to study generic aspects of cell differentiation but could also become a unique system in which to study how differentiation processes modulate overall tissue function.

Acknowledgements

Research work in the authors' laboratories was supported by: the Health Research Council of New Zealand, the Marsden Fund (NZ), the Wellcome Trust (UK), the Lotteries Grant Board (NZ), the University of Auckland Research Committee and the Auckland Medical Research Foundation.

References

- Menko AS. Lens epithelial cell differentiation. *Exp. Eye Res.* 2002; 75: 485-490.
- Bassnett S. Lens organelle degradation. *Exp. Eye Res.* 2002; 74: 1-6.
- Mathias RT, Rae JL, Baldo GJ. Physiological properties of the normal lens. *Phys. Rev.* 1997; 77: 21-50.
- Donaldson P, Kistler J, Mathias RT. Molecular solutions to mammalian lens transparency. *News Phys. Sci.* 2001; 16: 118-123.
- Merriman-Smith BR, Krushinsky A, Kistler J, Donaldson PJ. Expression patterns for glucose transporters GLUT1 and GLUT3 in the normal rat lens and in models of diabetic cataract. *Invest. Ophthalmol. Vis. Sci.* 2003; 44: 3458-3466.
- Grey AC, Jacobs MD, Gonen T, Kistler J, Donaldson PJ. Insertion of MP20 into lens fibre cell plasma membranes correlates with the formation of an extracellular diffusion barrier. *Exp. Eye Res.* 2003; 77: 567-574.
- Young MA, Tunstall MJ, Kistler J, Donaldson PJ. Blocking chloride channels in the rat lens: Localized changes in tissue hydration support the existence of a circulating chloride flux. *Invest. Ophthalmol. Vis. Sci.* 2000; 41: 3049-3055.
- Jacobs MD, Soeller C, Sisley AMG, Cannell MB, Donaldson P. Gap junction processing and redistribution revealed by quantitative optical measurements of connexin46 epitopes in the lens. *Invest. Ophthalmol. Vis. Sci.* 2004; 45: 191-199.
- Jacobs MD, Donaldson PJ, Cannell MB, Soeller C. Resolving morphology and antibody labeling over large distances in tissue sections. *Microsc. Res. Tech.* 2003; 62: 83-91.
- Bassnett S, Missey H, Vucemilo I. Molecular architecture of the lens fiber cell basal membrane complex. *J. Cell Sci.* 1999; 112: 2155-2165.
- Goodenough DA. The crystalline lens. A system networked by gap junctional intercellular communication. *Semin. Cell Biol.* 1992; 3: 49-58.
- Willecke K, Eiberger J, Degen J et al. Structural and functional diversity of connexin genes in the mouse and human genome. *J. Biol. Chem.* 2002; 277: 725-737.
- Paul DL, Ebihara L, Takemoto LJ, Swenson KI, Goodenough DA. Connexin46, a novel lens gap junction protein, induces voltage-gated currents in nonjunctional plasma membrane of *Xenopus* oocytes. *J. Cell Biol.* 1991; 115: 1077-1089.
- White TW, Bruzzone R, Goodenough DA, Paul DL. Mouse Cx50, a functional member of the connexin family of gap junction proteins, is the lens fiber protein, MP70. *Mol. Biol. Cell* 1992; 3: 711-720.
- Gao J, Sun X, Yatsula V, Wymore RS, Mathias RT. Isoform specific function and distribution of Na/K pumps in the frog lens epithelium. *J. Membr. Biol.* 2000; 178: 89-101.
- Gruijters WTM, Kistler J, Bullivant S. Formation, distribution and dissociation of intercellular junctions in the lens. *J. Cell. Sci.* 1987; 88: 351-359.
- Baldo GJ, Mathias RT. Spatial variations in membrane properties in the intact rat lens. *Biophys. J.* 1992; 63: 518-29.
- Gong XH, Baldo GJ, Kumar NM, Gilula NB, Mathias RT. Gap junctional coupling in lenses lacking alpha(3) connexin. *Proc. Nat. Acad. Sci.* 1998; 95: 15303-15308.

19. Tenbroek E, Arneson M, Jarvis L, Louis C. The distribution of the fiber cell intrinsic membrane proteins MP20 and connexin46 in the bovine lens. *J. Cell Sci.* 1992; 103: 245-57.
20. Kistler J, Bullivant S. Protein processing in lens intercellular junctions: cleavage of MP70 to MP38. *Invest. Ophthalmol. Vis. Sci.* 1987; 28: 1687-1692.
21. Lin JS, Fitzgerald S, Dong YM, Knight C, Donaldson P, Kistler J. Processing of the gap junction protein connexin50 in the ocular lens is accomplished by calpain. *Eur. J. Cell Biol.* 1997; 73: 141-149.
22. Lin JS, Eckert R, Kistler J, Donaldson P. Spatial differences in gap junction gating in the lens are a consequence of connexin cleavage. *Eur. J. Cell Biol.* 1998; 76: 246-250.
23. Berman ER. *Biochemistry of the Eye*. New York: Plenum Press, 1991.
24. Merriman-Smith R, Donaldson P, Kistler J. Differential expression of facilitative glucose transporters GLUT1 and GLUT3 in the lens. *Invest. Ophthalmol. Vis. Sci.* 1999; 40: 3224-3230.
25. Arneson ML, Louis CF. Structural Arrangement Of Lens Fiber Cell Plasma Membrane Protein Mp20. *Exp. Eye Res.* 1998; 66: 495-509.
26. Gonen T, Grey AC, Jacobs MD, Donaldson PJ, Kistler J. MP20, the second most abundant lens membrane protein and member of the tetraspanin superfamily, joins the list of ligands of galectin-3. *BMC Cell Biol.* 2001;17.
27. Perillo NL, Marcus ME, Baum LG. Galectins: versatile modulators of cell adhesion, cell proliferation, and cell death. *J. Mol. Med.* 1998; 76: 402-412.

Received 22 June 2004, in revised form 23 July 2004.

Accepted 24 July 2004.

©P.J. Donaldson 2004.

Author for correspondence:

Paul Donaldson

Department of Physiology

School of Medical Sciences

University of Auckland

Private Bag 92019

Auckland, New Zealand

Phone: +64 9 3737599

Fax: +64 9 3737499

E-mail: p.donaldson@auckland.ac.nz